Rising from the ashes: treatments stabilize carbon storage in California's frequent-fire forests

Ethan Yackulic[1]*[†], Micah Elias[2], Joe Shannon[3],
Sophie Gilbert[3,4], Michael Koontz[3†], Spencer Plumb[5],
Matthew Sloggy[6] and Katharyn Duffy[1,3]*

[1]School of Informatics, Computing and Cyber Systems, Northern Arizona University, Flagstaff, AZ,
United States, [2]Blue Forest, Sacramento, CA, United States, [3]Vibrant Planet, Truckee, CA, United States,
[4]University of Idaho, Moscow, ID, United States, [5]Verra, Program Development and Innovation,
Washington, DC, United States, [6]USFS Pacific Southwest Research Station, Albany, CA, United States

The stability of seasonally dry Western mixed-conifer forests is threatened by the history of fire suppression, logging, and now increasing climate-driven aridity. Durable aboveground carbon storage in living trees—a key ecosystem service of these fire-adapted forests—is at risk due to the disruption of natural fire cycles. Restoring the relationship between fire and forest structure is essential for long-term resilience. Fuel and density reduction treatments can help reestablish this balance by reducing fire severity and enhancing forest function.

We evaluated the effectiveness of 216 thinning treatments implemented across California's Central Sierra Nevada mountain range (2015−2023) using a natural experimental design and a novel matching framework. Treatment effects were measured using a dynamic baseline which represents the expected trajectory of a treated site had it remained untreated, accounting for local climate, vegetation, and disturbance conditions. Treatments reduced average fire severity by 32% and the prevalence of high-severity fire by 88%. Larger treatments (>6 ha) were especially effective, seemingly acting as fuel breaks when located near fire perimeters (<250 m). Notably, treated areas continued to sequester and retain carbon during the extreme 2020 drought, while untreated areas declined. Despite intentional biomass removal, carbon levels in nearly 75% of treated forests matched or exceeded baseline levels by year seven, with an average increase of 12.8 ± 4.7 Mg C ha^{-1}.

These results highlight the role of treatments in restoring resilient forest structures, reducing fire severity and drought mortality, and effectively stabilizing live carbon pools. This work provides support for landscape-scale management frameworks in fire-adapted forest ecosystems across the western U.S. in a future of intensifying aridity and stochastic fire occurrence.

Introduction

Seasonally dry mixed-conifer forests in California are adapted to frequent, low-severity fire and are more likely to persist under this fire regime (Safford and Stevens, 2017). These fires maintain function and health by clearing understory vegetation, cycling nutrients, and creating ecological niches for keystone species (Kelly and Brotons, 2017). Further, this type of functional fire enhances the regenerative capacity of many species, facilitating seed germination and resprouting (Savage and Mast, 2005; Ouzts et al., 2015). These forests are also subject to frequent drought, owing to the Mediterranean climate of their habitat (Safford and Stevens, 2017). The amount and spatial arrangement of biomass in seasonally dry mixed-conifer forests reflects their historical relationship with fire and drought. In these disturbance-adapted systems, carrying capacity is shaped by episodic events (Hurteau et al., 2024), competition among trees is relatively low (North et al., 2022), and structural complexity is common – with individual trees, clumps, and openings typically occurring at scales of 0.5 to several acres (Larson and Churchill, 2012).

Historic harvest, coupled with more than a century of fire suppression, has resulted in overstocked forest stands and a loss of spatial heterogeneity, rendering these forests more vulnerable to uncharacteristic and often catastrophic disturbance (Arno et al., 1995; Hessburg et al., 2015; Hessburg et al., 2019; Koontz et al., 2020). Climate change is exacerbating this threat through the increasing prevalence of hot droughts (Millar and Stephenson, 2015), which impose hydraulic and carbohydrate stress on trees (McDowell et al., 2008), increasing their susceptibility to disease and insect infestation (Dale et al., 2001; Bentz et al., 2010; Parks et al., 2016; Fettig et al., 2019; Koontz et al., 2021). Elevated drought- and insect-related mortality contributes to fuel accumulation and an abundance of dead biomass, triggering reinforcing cycles that intensify fire behavior when ignitions occur. Consequently, contemporary wildfires burn with greater intensity and contagion, making them increasingly difficult to suppress or control (Steel et al., 2018; Parks et al., 2023). This combination of land management legacies and climate effects disrupts the ecological processes that once stabilized these systems and threatens the long-term persistence of fire-adapted forests. Uncharacteristic wildfire followed by regeneration failure can drive long-term transitions to grasslands and shrublands (Stevens-Rumann et al., 2018; Davis et al., 2019; Coop et al., 2020; Davis et al., 2023), thereby lowering the landscape's carbon storage potential (Coop et al., 2016; Parks et al., 2019a).

Addressing the challenges posed by climate-amplified fire severity to forest resilience requires restoring the functional relationship between fire-adapted forests and natural disturbances. Targeted stand density reduction, particularly when combined with fuel reduction, offers a critical pathway to reestablish this balance. These proactive management strategies focus on reducing surface fuels, decreasing stem density, and targeting ladder fuels, thereby restoring forest structure to support the ecologically functional role of fire (Brown et al., 2004). While evidence increasingly supports the effectiveness of density reduction treatments in restoring forest function and mitigating wildfire severity (Davis et al., 2024; Figure 1), the carbon implications of these interventions remain contentious (Campbell et al., 2012; Law et al., 2022;

Hunter and Taylor, 2022). This debate is compounded by the modern intensification of wildfire severity, shifting climatic conditions, and the inherent difficulties in developing appropriate counterfactual comparisons necessary for robust evaluations.

The retention and stability of aboveground live carbon (hereafter "carbon") within these ecosystems can serve as vital proxies for the presence and function of forests, and also underpins their role as carbon sinks and contributors to climate resilience (Hurteau et al., 2019). Forest carbon storage has emerged as an "ecosystem service" with a developing environmental market, potentially increasing the pace and scale of management by unlocking new pools of project finance (Elias et al., 2025). Many private entities, either to comply with regulations or to meet voluntary, self-imposed targets, are seeking to offset or otherwise reduce their carbon footprint. Carbon sequestration through improved forest management is one potential source of these offsets, but durability of stored carbon in fire-prone ecosystems is seen as a major risk to the success of these efforts and resulting environmental markets, both domestically (e.g., California risk buffer pools; Badgley et al., 2022), and internationally (Chu et al., 2023). To address this challenge, new carbon accounting methodologies propose crediting fuel reduction treatments for enhancing long-term carbon stability. If validated, these approaches could expand market-based funding for forest management. Thus, durable carbon sequestration is critical not only for ecological resilience but also for advancing conservation finance and payments for ecosystem services.

In this study, we use a natural experimental design–comparing treated and untreated forest areas–to evaluate the durability of carbon storage following fuels treatments. A key facet of our approach is the application of dynamic baselines, which are increasingly considered the "gold standard" in forest carbon monitoring because they provide observation-based (*ex post*) estimates of intervention effectiveness and avoid the worst perils of static forecasts or biased site selection (Battocletti et al., 2024). The most recent implementations of dynamic baselines use a direct or weighted difference-in-differences approach, comparing project outcomes to a matched control region over time. Control regions can consist of a pool of potential sample points (VM0045 Methodology for Improved Forest Management Using Dynamic Matched Baselines from National Forest Inventories, v1.1), representative areas of the approximate size of the project area (West et al., 2023), or census-style reference regions that are many multiples the size of the project area (VM0047 Afforestation, Reforestation, and Revegetation, v1.0). These options vary in interpretability, sampling assumptions, and implementation feasibility across spatial extents. Regardless of the approach, the accuracy and precision of dynamic baseline assessments critically depend on the quality of the selected controls.

Here, we apply a census-based dynamic baseline approach to test the hypothesis that thinning treatments in California's central Sierra Nevada enhance forest stability and increase aboveground live carbon retention relative to untreated areas. We specifically selected the census-based method for its robustness in enabling rigorous matching of pre-treatment conditions–particularly carbon stocks, climate, and topography–at landscape scales. By matching treatment and reference areas based on pre-treatment carbon, which strongly influences wildfire severity through fuel availability (Dillon, 2015; Parks et al., 2018), we directly evaluate treatment
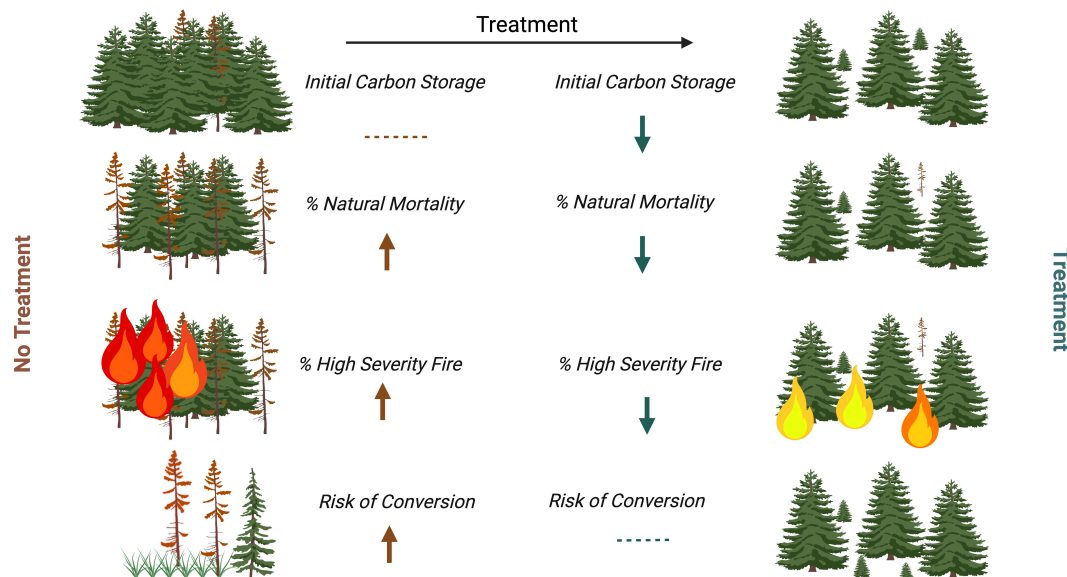
FIGURE 1
Conceptual model of aboveground live carbon fluxes leading to reduced durability of storage in an overstocked conifer forest. In the treatment scenario, an initial decrease in carbon storage occurs due to removal of woody material. However, these removals reduce the rate of natural mortality due to competition, disease and insect predation, as well as high severity of fire through the removal of understory fuels. This mitigation reduces the likelihood of forest conversion to lower-carbon ecosystems (e.g., grassland or shrubland). In contrast, untreated forests maintain initial carbon levels but face higher risks of mortality and severe fire, increasing the probability of conversion and carbon loss. Created by BioRender.

effectiveness under realistic disturbance conditions. Additionally, because our analysis spans the extreme fire years of 2020–2021, it provides a stringent test of whether fuel treatments effectively stabilize carbon storage and mitigate compounding risks from severe fire and drought.

Materials and methods

Study site

This study focuses on California's Central Sierra Nevada, a region critical to wildfire management and climate resilience due to its ecological diversity and sensitivity to climate-amplified disturbances (Figure 2). Over the past two decades, this area has experienced increasingly severe and expansive wildfires (Steel et al., 2018), compounded by severe drought conditions (Williams et al., 2023). Together, these stressors have elevated the risk of forest degradation, mortality, and potential conversion to non-forest ecosystems (Coop et al., 2022; Safford et al., 2022).

The Central Sierra Nevada is representative of seasonally dry, fire-prone forests across the western United States, sharing common challenges of high wildfire risk and ecological instability. Our study area spans approximately 6.3 million acres, encompassing six Level IV Ecoregions (Omernik and Griffith, 2014) characterized by mixed-conifer forest communities, steep topography, and diverse wildfire hazard conditions. These varied ecological settings provide a robust landscape for evaluating thinning treatment effectiveness. Less than one-third of the study area is privately owned, and approximately 11% lies within the wildland-urban interface (WUI; Radeloff et al., 2023). Public lands

in the study region are primarily managed by the U.S. Forest Service (~61%) and the Bureau of Land Management (~19%; CalFire, 2024).

Conifer forests dominate the undeveloped portions of the study area (~74%), with shrub (~14%) and hardwood (~5%) densities increasing at lower elevations (Landfire, 2016). Common conifer species include Jeffrey pine (*P. jeffreyi*), sugar pine (*P. lambertiana*), ponderosa pine (*Pinus ponderosa*), and incense cedar (*Calocedrus decurrens*) (Fites-Kaufman et al., 2007). Historically, these forest types experienced frequent, low- to moderate-severity fire regimes (Van de Water and Safford, 2011; Safford and Stevens, 2017).

Natural experimental design

We assessed treatment effectiveness using a natural experimental design embedded within a difference-in-differences framework (Ashenfelter and Card, 1984). This method compares temporal changes in treated areas against matched untreated controls (Reference Regions; RRs), assuming similar trajectories in the absence of intervention (Fick et al., 2021). To strengthen this assumption and account for potential selection biases, we also developed "placebo treatments"–untreated sites that met all criteria for treatment selection–paired with corresponding placebo reference regions (Table 1).

The counterfactual design was structured around four groups:

1. Treatments: Areas that underwent thinning interventions, enabling direct measurement of treatment impacts.
2. Treatment Reference Regions (Treatment RRs): Broad, spatially dispersed regions representing untreated conditions, enabling robust comparisons across a larger landscape.

FIGURE 2
Map of the level IV ecoregions in the Central Sierra Nevada region. Treatments from 2016 that were included in this study are shown in orange. Major fire footprints from the Caldor, North Complex and Dixie 2020 and 2021 wildfires are shown in black outlines. The distribution of treatment elevations are shown in the inset graph (bottom right).
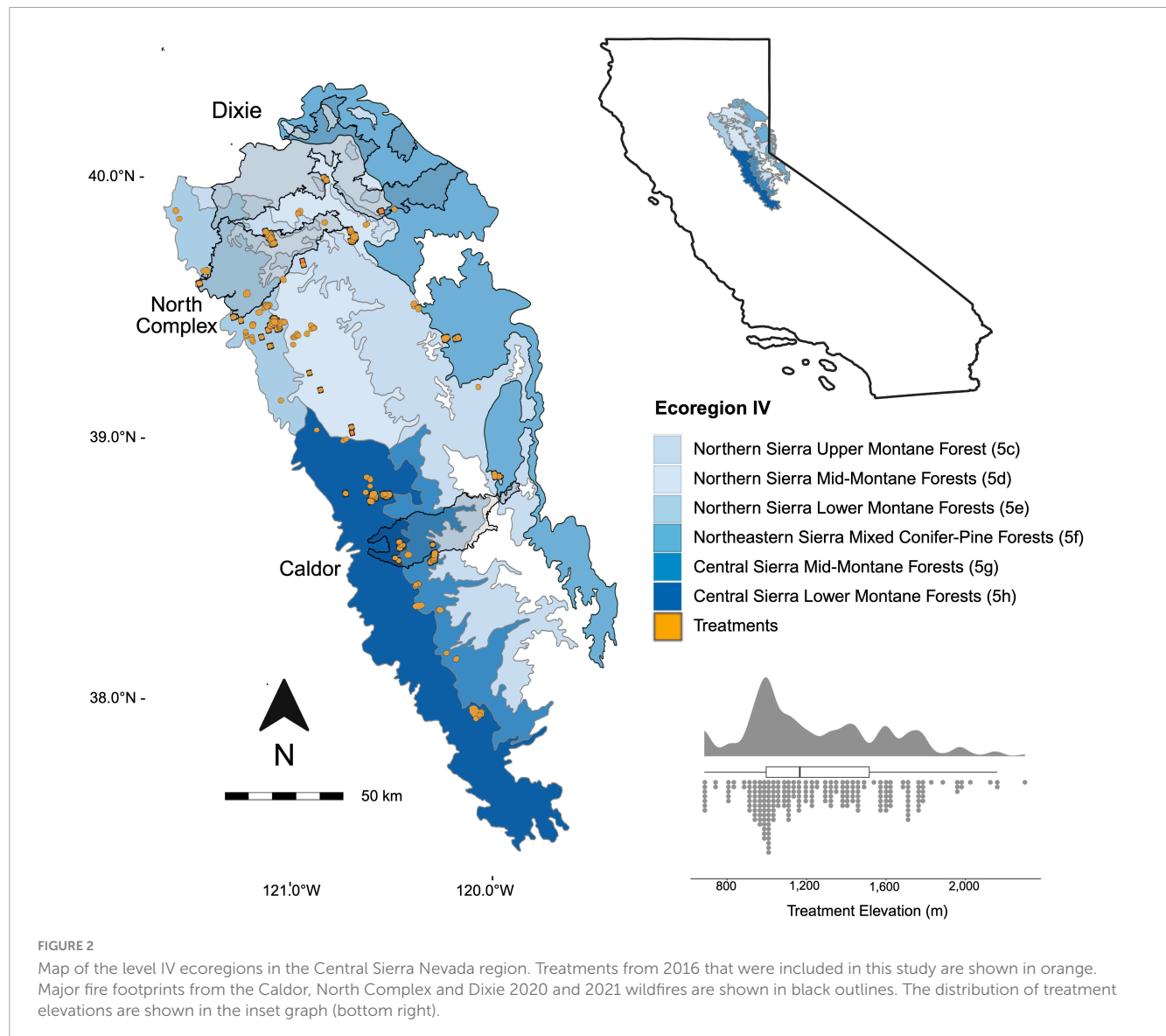
3. Placebo Treatments: Untreated areas that met treatment criteria for thinning interventions, designed to account for inherent site characteristics that could otherwise confound treatment effects. A replicate placebo treatment is assigned to each actual treatment and mimics the same carbon distribution and spatial configuration, placed elsewhere in the applicable landscape (Supplementary Figure 1).

4. Placebo Reference Regions (Placebo RRs): Controls for placebo treatments, developed using the same census-based matching approach as treatment reference regions.

The inclusion of placebo treatments and placebo reference regions enhances the counterfactual design by addressing two critical considerations:

1. Selection Bias: Placebo treatments allow us to test whether the observed effects are due to site-specific characteristics that dictate how managers select treatment areas, rather than thinning interventions themselves.

2. Stochastic Variability: Placebo reference regions provide a broader ecological and geographical basis for assessing variability in untreated conditions.

The inclusion of placebo treatments and their reference regions strengthens the robustness of the counterfactual framework, reducing uncertainties and bolstering confidence in the causal nature of resulting signals. This layered approach serves as a proxy for pre-treatment match quality evaluation and ensures that the measured outcomes accurately reflect the effects of thinning treatments, rather than confounding factors, making it a critical component of this study's methodology.

Treatment selection

We limited our analysis to treatments that were implemented in 2016 such that we could accurately track pre-treatment carbon storage and capture post-treatment recovery. To ensure that

TABLE 1 Summary of treatment and control groups used for hypothesis testing. Each group has 216 observations.

Hypothesis Group	Treatment	Purpose	*Cumulative* size (acres)
Interventions	Y	Measurement of intervention effect	14,000
Reference regions	N	Intervention counterfactual; spatially-dispersed	1,228,000
Placebo interventions	N	Placebo control of intervention effect; spatially-concentrated to represent interventions	12,000
Placebo reference regions	N	Placebo intervention counterfactual; spatially-dispersed	850,000

treatments (*a*) occurred, (*b*) existed within fire-prone areas and (*c*) removed an observable amount of carbon, we used this criteria to select commercial thinning treatments (ensuring *a* and *c*) from an analysis-ready version of the Forest Activity Tracking System (FACTS) and CALFIRE databases (Knight et al., 2022). These treatments carry the most significant biomass removal, and thus enable a more extreme example of carbon costs to evaluate potential return. We required that project pixels were forested prior to treatment (Existing vegetation cover; 20–100% forested; Landfire, 2014), conifer-dominated (Existing vegetation type; Landfire, 2016), and at risk of wildfire (Wildfire hazard potential; "high" or "very high"; Dillon, 2015). In an effort to capture the realized implementation of fuel reduction treatments we did not add any additional treatment restrictions (i.e., intensity of treatment, presence/absence of follow-up prescriptions). Within the Central Sierra region, we identified 216 unique thinning treatments totaling ∼ 14,000 acres, with 101 (∼8,000 acres) treatments receiving subsequent surface fuel release via pile burning, prescribed burn, or biomass removal in the years 2017–2020. A unique reference region

was generated to match each thinning treatment, resulting in 216 reference regions total.
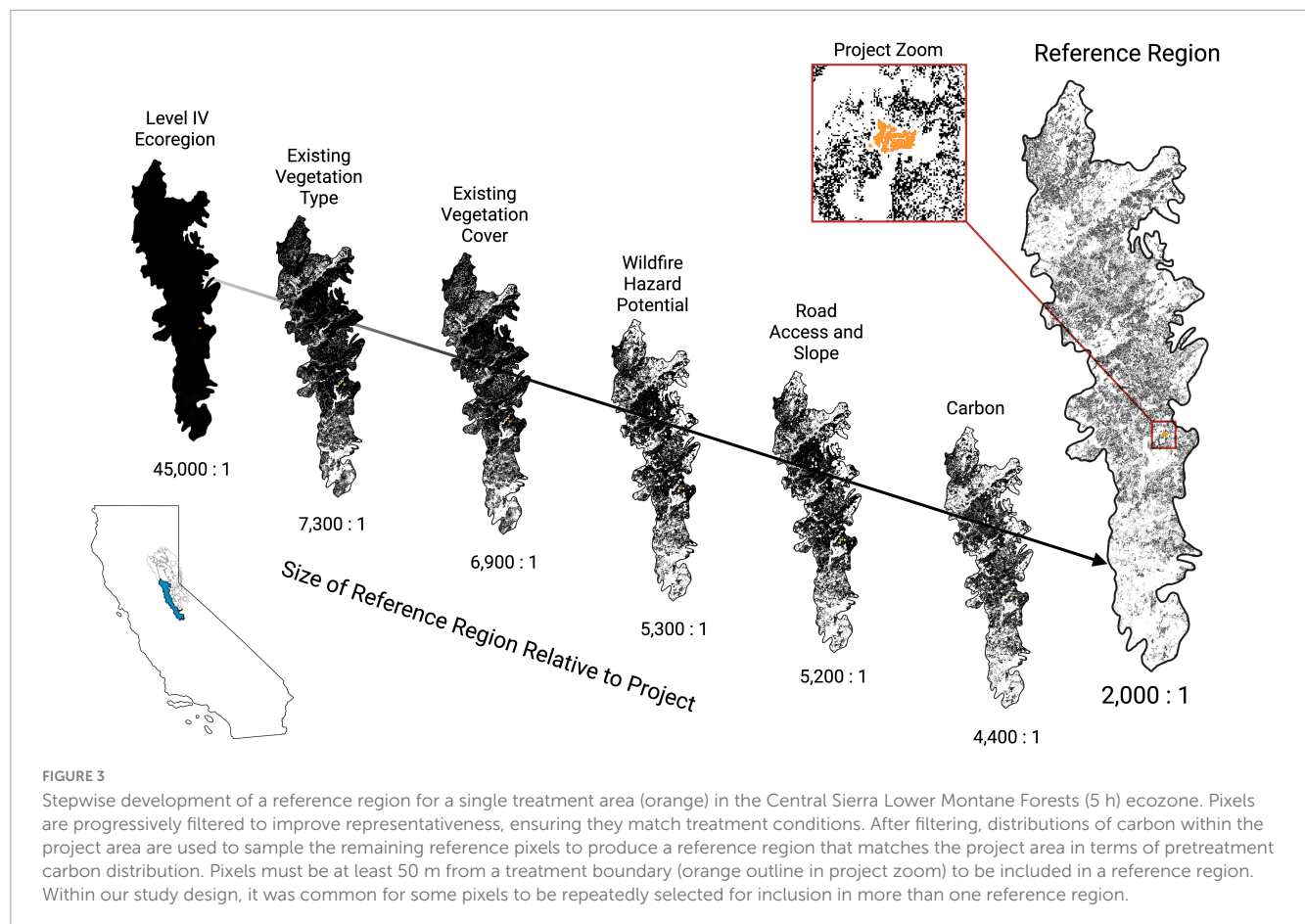
Reference region development

To create effective controls for this analysis, we developed a census-based matching approach that makes use of publicly available datasets and clear matching rules. Reference region attributes were matched at time 0 (year prior to treatment intervention), while outcome variables (carbon, fire severity) were observed at time 0 and annually thereafter. Reference regions then served as the static control group for our dynamic baseline approach (see Dynamic Baseline). By restricting all matching to pretreatment datasets (Table 2), we ensured that no post-treatment information biased control selection or interpretation.

The census-based approach for developing reference regions functions as a series of successive filters, systematically narrowing potential reference areas to align with the characteristics of the intervention area prior to intervention (Figure 3). We started with the entire geographic area and applied successive filters based on ecological, geographical, and fire-hazard criteria.

1. Ecoregion Matching: Treatment areas were first matched to their respective Level IV Ecoregions to ensure ecological consistency (Omernik and Griffith, 2014). Ecoregions are defined based on enduring ecosystem components, such as soils, forest types, and elevation, and provide a consistent framework for comparisons. When treatment boundaries spanned multiple ecoregions, multiple RRs were developed.
2. Pixel-Level Filtering: Within each ecoregion, pixels were retained if they:

   a. Contained at least 20% existing vegetation cover (EVC; Landfire, 2014), matching the observed range in treatment areas.
   b. Were classified as "Conifer" within the existing vegetation type (EVT) physiognomy grouping (Landfire, 2016).
   c. Were classified as having "high" or "very high" wildfire hazard potential (WHP; Dillon, 2015) (see Treatment Selection).

TABLE 2 Datasets used for developing reference regions (RR), including sources, filtering criteria, and spatial resolutions.

Dataset	Source	Filtering criteria	Year	Resolution
IV Ecoregion	EPA	Present in >5% of treatment area	2013	125 m
Existing vegetation type (EVT)	LANDFIRE	Treatment area and RR filtered to physiognomy grouping of "Conifer."	2016	30 m
Wildfire hazard potential (WHP)	LANDFIRE	"High" or "very high"	2014	270 m
National transportation dataset	USGS	<600 m from road and slope <35 or <300 m from road and slope is between 35 and 50°	2024	30 m
Digital elevation model	USGS		2023	1 m
Existing vegetation cover (EVC)	LANDFIRE	Treatment area must be >20% forested. RR is filtered to the range of values present in the treatment area. Max quantile match of treatment area distribution.	2014	30 m
Aboveground live biomass	NASA CMS	Filtered to exclude values outside the range present in the treatment area. Max quantile match of treatment area distribution	2015–2023	30 m

FIGURE 3
Stepwise development of a reference region for a single treatment area (orange) in the Central Sierra Lower Montane Forests (5 h) ecozone. Pixels are progressively filtered to improve representativeness, ensuring they match treatment conditions. After filtering, distributions of carbon within the project area are used to sample the remaining reference pixels to produce a reference region that matches the project area in terms of pretreatment carbon distribution. Pixels must be at least 50 m from a treatment boundary (orange outline in project zoom) to be included in a reference region. Within our study design, it was common for some pixels to be repeatedly selected for inclusion in more than one reference region.

d. Met treatment feasibility criteria, including accessibility (e.g., proximity to roads) and topographic suitability (e.g., slopes $< 50°$).

3. Carbon and EVC Distribution Matching: Sample weights were computed based on the pre-treatment distribution of carbon (along 5 MgC/ha bins) and EVC (10% cover bins) to avoid biasing our results based on differences in pre-treatment carbon and EVC between the intervention and reference areas. This results in a reference region that is n times larger than the treatment with a statistically equivalent distribution of pre-treatment carbon stocks.

This selection process produced a reference region (Figure 3; far right panel) that was several orders of magnitude larger than the treatment area, but matched in terms of forest type, wildfire vulnerability, and likelihood of treatment. Systematic differences in pretreatment carbon distributions between the treatment area and reference region would result in biased post-treatment results.

Placebo treatment development

Observational studies, including natural experiments, are inherently vulnerable to selection bias – systematic differences between treated areas and controls that could confound results (Fick et al., 2021). To evaluate potential bias, we created 216

"placebo" treatment polygons (placebos) throughout the Central Sierra region. These placebo treatments (i.e., "pseudo projects"; Golmant et al., 2023) were randomly placed throughout the region in locations where treatment did not occur, but would have been likely based on the criteria listed in Table 2. We then produced reference regions for each placebo treatment as described above. The difference between the placebo treatment polygons and their respective reference regions provides a measure of match quality, which we use as a proxy for systematic selection bias effects. The difference between placebo treatment polygons and intervention polygons enable evaluation of the difference between the effects of treatment and fire (intervention polygons) and the effects of fire alone (placebo treatment polygons).

Dynamic baseline

We quantified changes in aboveground live carbon using annual estimates of forest biomass from the NASA Carbon Monitoring System (CMS), a 30 m resolution, satellite-derived dataset validated with FIA field plots (Kennedy et al., 2024). Estimates from 2016 through 2023 were used to evaluate changes in carbon stocks within treatment intervention areas relative to matched reference region (RR) controls. The utility of satellite-derived aboveground biomass data for capturing both carbon stock and flux has been well-demonstrated in operational systems (e.g., Kennedy et al., 2018), which show the value of integrating
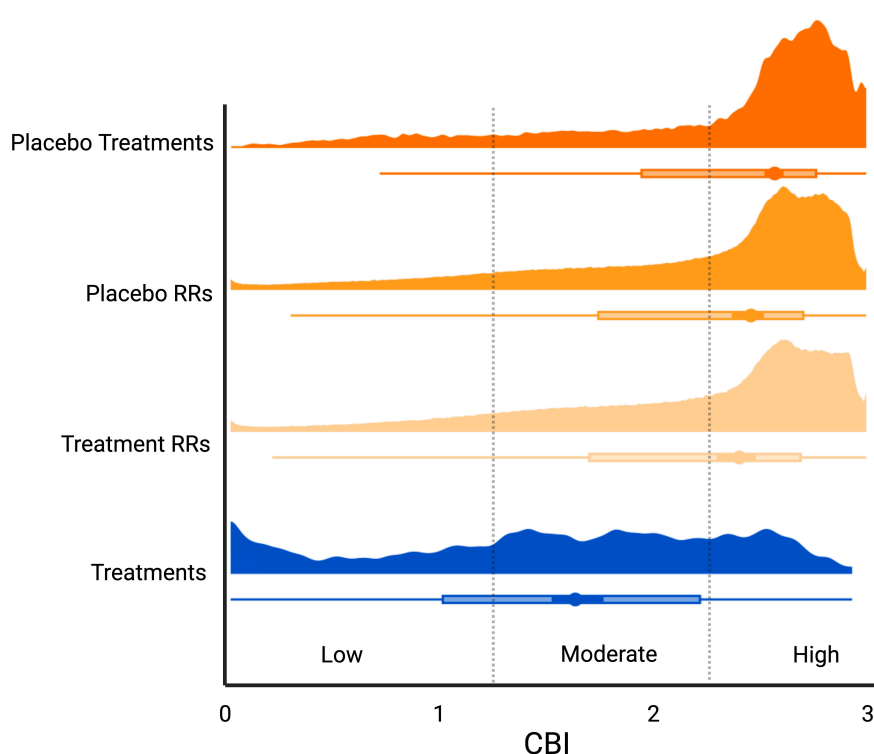
FIGURE 4

Comparison of fire severity distributions (composite burn index; CBI) across 2016 treatment polygons and untreated control areas (discrete placebo polygons and dispersed reference regions (RRs)). Fire severity distribution of untreated areas is right-skewed, dominated by high-severity fire. In contrast, treated areas exhibit a more even distribution across severity classes, indicating a shift toward mixed-severity fire. Dots and lines represent means and confidence intervals for each group.

FIA plots with time-series Landsat imagery and statistical models to track disturbance and regrowth processes annually at management-relevant scales. Biomass estimates were converted to metric tons of aboveground live carbon storage per hectare (MtC ha^{-1}) by applying a standard 0.5 conversion factor (i.e., carbon = 0.5 × biomass), following IPCC guidelines (IPCC, 2006). Carbon dynamics in our analysis were assessed in conjunction with remotely sensed fire severity metrics, including Composite burn index (CBI) and the proportion of area burned. Comparisons focused on pre-treatment (2015), treatment year (2016) and post-treatment observations (2017–2023).

Composite burn index values were computed and bias-corrected for all fires in the study area using the remote sensing model developed by Parks et al. (2019b). This model applies a spatially cross-validated random forest algorithm (Breiman, 2001), trained with field measurements, to predict CBI from pre- and post-fire spectral indices, climatic water deficit normals, and latitude. Pre- and post-fire mean composites of spectral indices are created using imagery from the June 1 to September 15 period. Pre-fire mean composites use imagery from the year prior to the fire and post-fire mean composites use imagery from the year after the fire in order to ensure that no post-fire images contribute to pre-fire mean composites and vice-versa. These additional covariates used to model CBI provide regional context and improve the ecological interpretability of severity estimates, especially in heterogeneous landscapes where treatment effects span climatic and topographic gradients.

Fire perimeters were compiled from Welty and Jeffries (2021) and the WFMRDA Interagency Wildland Fire Perimeter History (2022), then dissolved by year to avoid duplication of fire events. To evaluate treatment effects across severity gradients, we stratified observations into the following CBI classes: unburned ($0 \leq$ CBI < 0.1), low severity ($0.1 \leq$ CBI < 1.25), moderate severity ($1.25 \leq$ CBI < 2.25), and high severity ($2.25 \leq$ CBI ≤ 3.0). The spatial footprints of fire are generally large when compared to treatment areas, thus fire is generally entirely present, or absent, within treatments and placebo treatments (Supplementary Figure 2) (e.g., partially burned treatment units are generally rare, which might not be true if fires tended to be very small). Conversely, RRs are large enough for observed fire activity to vary spatially and dampen the stochastic signal of fire realized across a landscape. For comparisons, we aggregated all pixels within each group described in Table 1 to compare mean responses to treatment and fire (Figures 4, 5, 6, and Table 3). We also evaluated individual treatments and their RRs to determine treatment benefits (Figure 5; panel II). For each treatment area, we sampled an equal-sized replicate from the reference region to calculate t-tests. We repeated 10,000 random draws for each paired treatment - reference region to estimate mean differences and uncertainties.

We evaluated the role of treatment size in reducing wildfire severity by observing the effects of three major fires during our study period: Caldor, Dixie and North Complex fires (Figure 2). For treatments within 1 km of these fire perimeters, we used polygon locations to measure the closest distance between fire and treatment
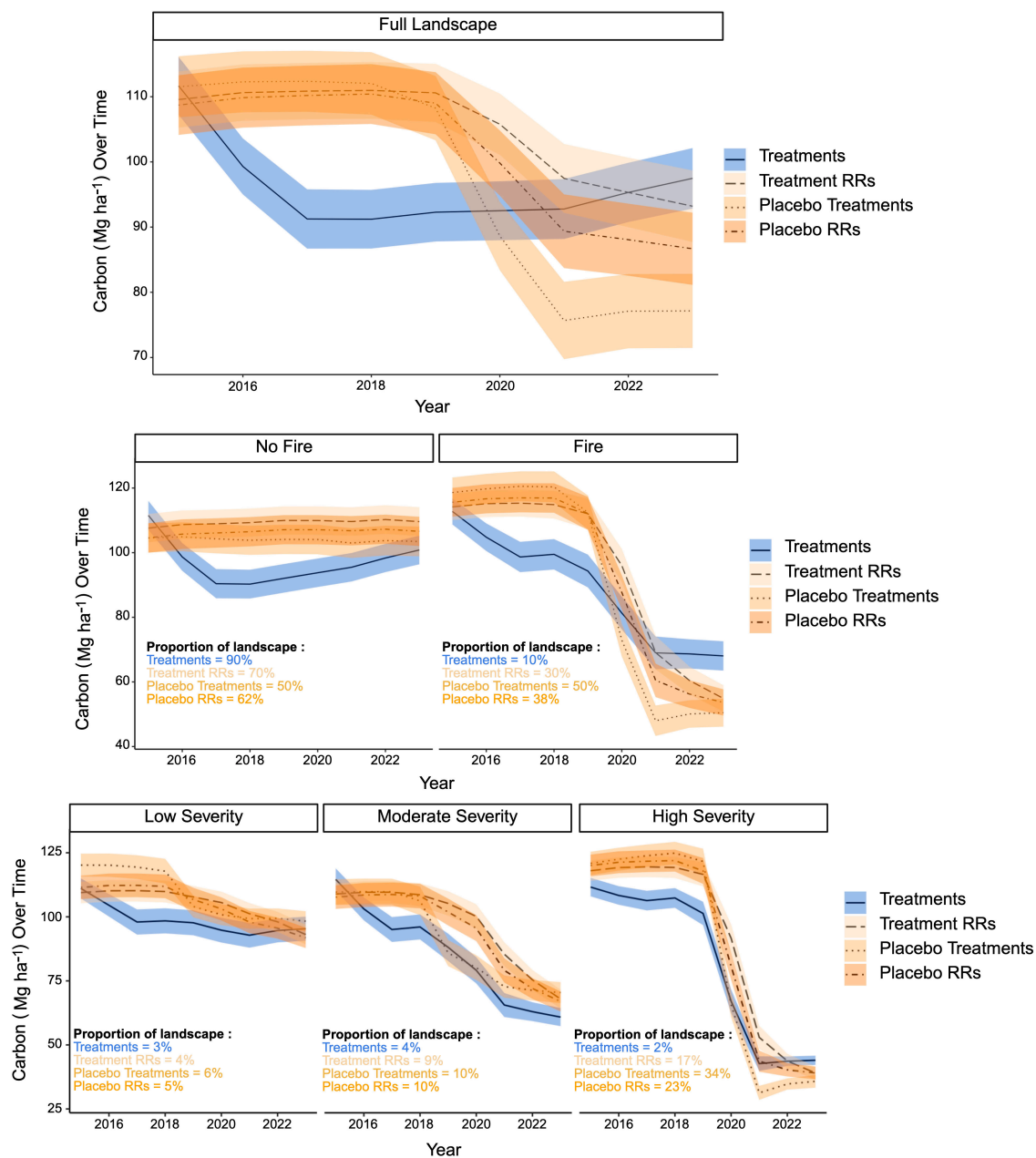
FIGURE 5
Time series of carbon change for treated and untreated groups (Treatment Reference Regions - Treatment RRs, Placebo Treatments, Placebo Reference Regions - Placebo RRs). The top panel displays annual carbon inventories across all groups for the entire landscape from 2015 to 2023. In the middle panel, the results are split into pixels that either experienced no fire or fire. Finally, the bottom panel explores how the patterns shown in the middle panel for "Fire" are split across different severity classes. Lines and colors display means and 95% confidence intervals for treatment and untreated groups. Despite similar trajectories of carbon loss across the three severity classes (bottom panel), treatments have a statistically significant difference in carbon responses to fire (middle panel), due to a lower frequency in the occurrence of high severity fire. Pixels that did not experience fire, however, were not distinctively different in terms of total carbon storage in 2023, despite the intentional removal of carbon recorded in 2016 and re-entry treatments.

perimeters (*terra* package; Hijmans, 2025) and used buffered fire perimeters to flag treatments that were directly adjacent to fire perimeters (≤250 m).

We further investigated treatments that experienced fire (40 intervention polygons) to determine whether treatment size influenced fire behavior. For treatments within 1 km of the Caldor, Dixie and North Complex fire perimeters, we used polygon locations to measure the closest distance to between fire and

treatment perimeters. We created a 250 m buffer around each treatment and recorded which buffered treatments intercepted a fire perimeter. A linear model was developed to determine whether treatment polygon size was correlated with treatment polygons that did or did not cross a fire perimeter. A separate linear model compared CBI measurements of treatment pixels with reference region pixels that lay directly outside of the treatment buffer.
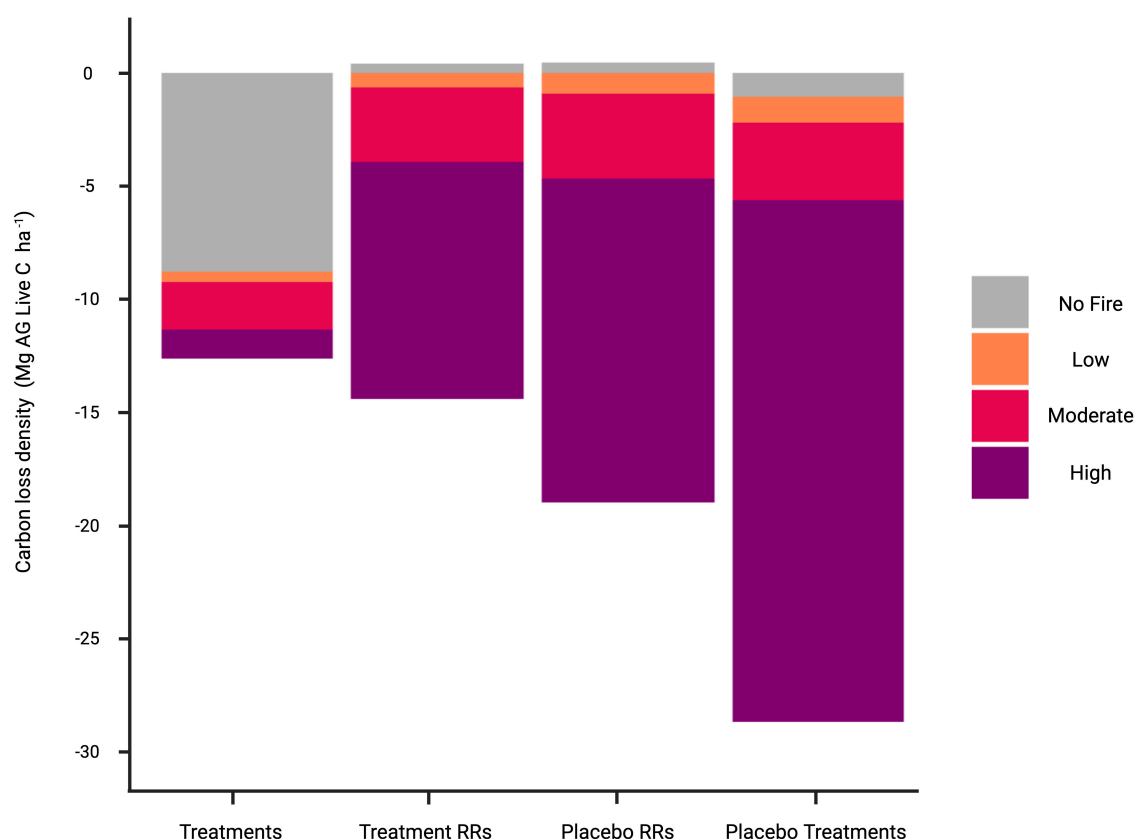
FIGURE 6
Contributions of different fire severity classes (including no fire) to carbon losses in the treatment and control groups from 2015 to 2023. Calculated as Δ carbon scaled by the % area for each group. Note differences in no fire and high-severity fire between treated (treatments) and untreated (Reference Regions - RRs and Placebo) groups. Treatment losses in the no fire scenario are almost entirely attributable to biomass removal during treatment, while high severity fire is the predominant source of losses in the control groups.

Significance testing

Bayesian generalized linear models were produced to examine differences in fire severity and carbon between each time step for each treatment - reference region grouping and within each severity category. By maintaining balanced observations across all groups (*n* = 216), this design ensures consistency in sample sizes, enabling statistically rigorous comparisons. We employed the Highest Density Interval-Region of Practical Equivalence (HDI-ROPE; *bayestestR* package; Makowski et al., 2019) test to identify where differences between groups were practically significant. This test is appropriate because, unlike *p*-values, significance determined by HDI-ROPE is not correlated with sample size and does not base significance on differences from zero. As the name suggests, the user is able to provide a range of values that are practically equivalent to zero effect. In our case, where the localized occurrence of fire or drought mortality may provide significant statistical noise, ROPE allows us to determine an acceptable range of random behavior. We followed standard procedures and set our ROPE range to equal ± 1 standard deviation of the 89% Highest Density Interval (Kruschke, 2018). This approach effectively allows for a conservative estimate of treatment effects compared to a reference region baseline.

Results

Fire effects

The reference regions developed for both treatments and placebo treatments were closely aligned in their fire exposure and severity metrics (Figure 4). Across the study period, 30% of treatment reference regions and 38% of placebo reference regions burned – an 8% difference. The proportions of low-, moderate-, and high-severity fire also showed minimal differences between treatment and placebo reference regions (Δ 1%, 1%, and 6%, respectively), with nearly identical mean CBI values (Δ 0.1%). Fire occurrence was highly variable across years, with more than 75% of all fire-affected pixels in both treated and untreated areas burning during the extreme 2020 and 2021 fire seasons (Supplementary Figure 3). Despite this variability, carbon loss patterns within severity classes remained consistent across all groups and time steps, with a maximum difference of only 3%.

Pooled placebo treatment observations closely matched reference regions in mean CBI (2.3 vs. 2.2) and the proportional distribution of low- (∼6% of the total landscape) and moderate-severity (∼10%) fire, which also align with independent assessments of severity fraction in the region (Steel et al., 2018, Williams et al., 2023). Placebo treatments exhibited higher
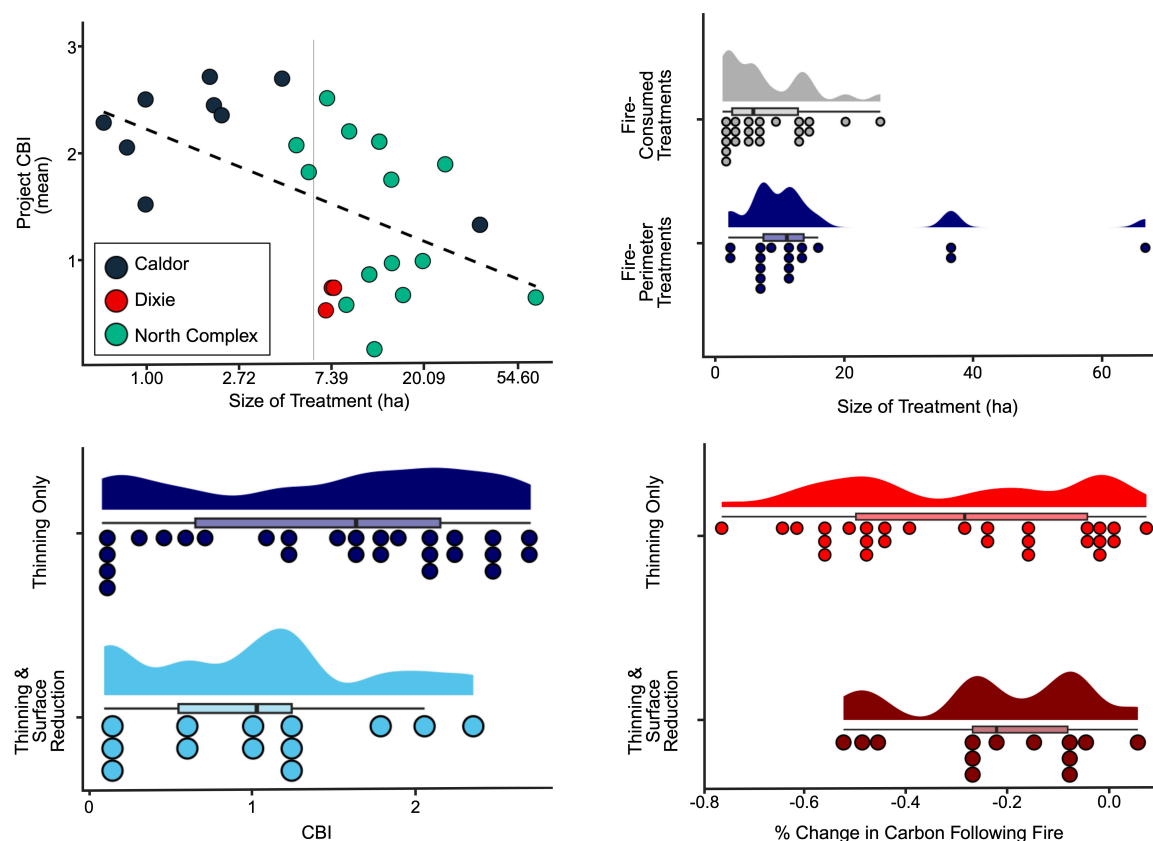
FIGURE 7

Effects of treatment size **(top panel)** and management reentry **(bottom panel)** on fire severity. The top left panel shows the relationship between mean CBI and treatment area (*x*-axis is log transformed with real units displayed) within burned projects, across three major fires (Caldor, Dixie, North Complex). The top right plot shows the relationship between size of treatment and position on the landscape; larger treatments were more likely to occur around the perimeters of fires, rather than being fully consumed. The bottom left panel shows that CBI significantly dropped in treatments that experienced an additional surface reduction treatment. Furthermore, these treatments stored more carbon following fire (bottom right panel).

frequencies of high-severity fire (∼34%) than both reference regions, reflecting realized contagion within contiguous tracts of forest that did not receive treatment (Table 3). Both placebo treatments and placebo reference regions exhibited equivalent burn severity distributions (Figure 4). In contrast, treatment intervention polygons displayed interannual variability in the proportion of area burned (Supplementary Figure 3). Notably, we observed redistributed fire severity toward lower intensities within the treatment polygons relative to all untreated control groups (treatment RRs, placebo RRs, and placebo treatments) (Figure 4). While high-severity fire dominated burned areas across all controls, treatment intervention polygons predominantly experienced mixed-severity fire (Figure 4). For clarity in subsequent sections, untreated observations are grouped together for comparison with treatment effects due to the similarity of behavior across all types of untreated groups.

Treatments experienced lower fire severity across the study area, with mean CBI reduced by ∼32% and high-severity fire frequency 88% lower compared to controls (Figures 5, 7, and Table 3). Treated areas experienced ∼90% less aboveground carbon loss from high-severity fire than untreated areas. Despite these reductions in high-severity outcomes, treatments exhibited similar proportions of low- and moderate-severity fire compared to untreated areas, treated areas had a more even spread of fire

across low, moderate, and high severities (a mixed-severity pattern) compared to the untreated areas, rather than fully excluding fire from the landscape.

The reduction in fire severity in treatment polygons relative to control areas is most notable in treatments greater than 6 hectares in area (Figure 7, top left panel). Of the 40 treatment boundaries that were exposed to wildfire, 18 occurred at or near (within 250 m) the fire perimeter (Figure 7, top right panel). We note that proximity to a fire perimeter (<250 m) was weakly correlated to larger treatment size ($R^2 = 0.10$, $p < 0.05$; Figure 7). In general, larger treatments experienced lower fire severity when compared to nearby reference region pixels (i.e., pixels that lie within 250 m of the treatment boundary; $R^2 = 0.45$, $p < 0.001$).

Carbon storage

Over the study period, there was a notably larger reduction in percent carbon in control areas relative to treated areas (top panel of Figure 5). In the years prior to extreme fire activity (2020 and 2021), treated areas lost significantly more carbon than controls, primarily due to biomass removal (top panel of Figure 5). However, 2020 and 2021 marked a drastic shift in treatment performance. These years were characterized by exceptionally large

TABLE 3 Summary statistics of carbon storage and fire severity across treatment types and their corresponding reference regions (italicized for untreated areas).

Subset	Group	μ2015	μ2016	μ2017	μ2018	μ2019	μ2020	μ2021	μ2022	μ2023	Δ 2015: 2023 (%)	Δ 2017: 2023 (%)	μCBI	% Area
All pixels	**Treatments**	112	99	91	91	92	93	93	95	97	−13	7	1.5	100
	Reference regions	110	**111**	**111**	**111**	**111**	106	**97**	95	**93**	**−15**	**−16**	**2.1**	100
	Placebo Treatments	112	**112**	**112**	**112**	**108**	89	**76**	**77**	77	**−31**	**−31**	**2.3**	100
	Placebo RRs	109	**110**	**110**	**110**	**109**	100	89	**88**	**87**	**−20**	**−21**	**2.2**	100
No fire	**Treatments**	112	99	90	90	92	94	95	98	101	−10	12	0	90
	Reference regions	**108**	**109**	**109**	**109**	**110**	**110**	**110**	**110**	110	**2**	**1**	0	70
	Placebo Treatments	**105**	**105**	**104**	**104**	**104**	**104**	**103**	**104**	104	**−1**	**0**	0	50
	Placebo RRs	**105**	**106**	**106**	**106**	**107**	**107**	**107**	**107**	**107**	**2**	**1**	0	62
Fire	**Treatments**	113	105	99	99	94	81	69	69	68	−40	−31	1.5	10
	Reference regions	114	**115**	**115**	**115**	**112**	**96**	69	**60**	**55**	**−52**	**−52**	**2.1**	30
	Placebo Treatments	**119**	**120**	**121**	**120**	**112**	73	**48**	**50**	**50**	**−57**	**−58**	**2.3**	50
	Placebo RRs	116	**117**	**117**	**117**	**112**	**88**	**60**	**56**	**54**	**−54**	**−54**	**2.2**	38
Low severity	**Treatments**	111	105	98	98	98	95	93	95	95	−14	−3	0.6	3
	Reference Regions	109	**110**	**110**	**110**	108	**106**	**101**	98	93	−15	**−16**	**0.8**	4
	Placebo Treatments	**120**	**120**	**119**	**118**	104	**101**	**99**	**99**	98	**−18**	**−18**	**0.8**	6
	Placebo RRs	111	**112**	**112**	**112**	107	103	98	96	92	**−18**	**−18**	**0.8**	5
Moderate severity	**Treatments**	115	103	95	96	88	79	66	63	61	−47	−36	1.7	4
	Reference regions	**109**	**110**	**110**	**109**	105	**100**	**85**	75	**68**	**−38**	**−38**	**1.8**	9
	Placebo Treatments	**110**	**110**	**110**	**106**	86	80	**73**	71	70	**−36**	**−36**	**1.8**	10
	Placebo RRs	**108**	**109**	**109**	**108**	102	**96**	79	72	67	**−38**	**−38**	**1.8**	10
High severity	**Treatments**	112	108	106	107	101	67	43	44	44	−61	−59	2.5	2
	Reference regions	**118**	**119**	**120**	**119**	**117**	**92**	**53**	44	**39**	**−67**	**−67**	**2.7**	17
	Placebo Treatments	**121**	**123**	**124**	**125**	**122**	66	**31**	**35**	**36**	**−70**	**−71**	**2.7**	34
	Placebo RRs	**120**	**121**	**122**	**122**	**118**	**81**	44	**40**	**39**	**−67**	**−68**	**2.7**	23

Metrics include mean values (μ; MtC ha^{-1}) and percent changes (Δ) across different time periods. The first panel presents data for all pixels, while subsequent panels detail subsets categorized by fire severity. Statistically significant differences from treatments are indicated in bold. Differences in columns 4–6 are relative to the stated timesteps (i.e., $[\mu^{t=2} - \mu^{t=1}]/\mu^{t=1}$).
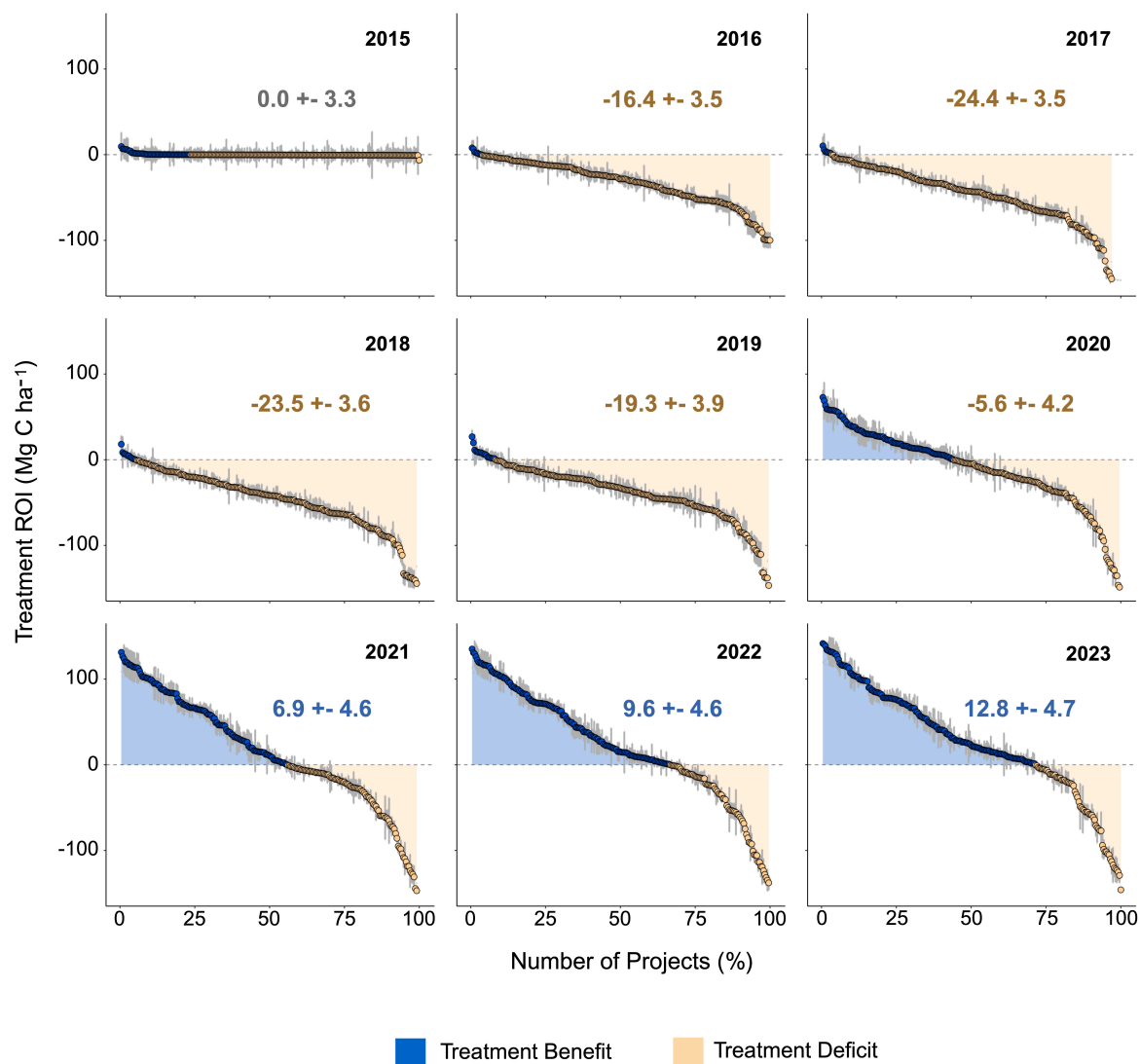
FIGURE 8
Time series of carbon change for individual treatment areas vs. their reference regions. Differences in carbon per hectare are calculated at each time step for each treatment area and its corresponding reference region. We compared each treatment with 1,000 iterations of equal sample size draws from their reference region to measure uncertainty. Blue (yellow) dots depict treatment areas that have a net positive (negative) carbon response relative to their reference region. Text values display cumulative treatment ROI at each time step.

and severe wildfires, with more than 87% of all burned pixels in the study occurring during this 2-year window (Supplementary Figure 3). During this period, treated areas exhibited markedly greater resistance to fire-related carbon loss than controls (middle-right panel of Figure 5). This pattern stems from differences in the distribution of fire severity classes across groups (bottom panels of Figures 4, 7). While carbon losses per severity class were similar between treatments and controls, the overall carbon impact was shaped by the proportion of area that burned at low, moderate, or high severity (Figure 6). Notably, carbon storage in treated areas were ∼25% lower than in control areas by 2019, reflecting intentional biomass removal during treatment. To isolate the effect of fire, we also compared unburned areas within each treatment-control pairing (middle-left panel of Figure 5). In controls, net carbon storage remained relatively static from 2015 to 2023, while treated areas showed a steady post-treatment increase in carbon

storage beginning around 2017 (Table 3). By 2023, we found no statistically significant differences in carbon storage between treated and control groups–despite the fact that treatments were the only group to undergo biomass removal.

The timing and magnitude of carbon loss differed significantly between treated and control areas (Figure 5 and Table 3). The majority of total carbon loss over the study period in treated areas coincided with biomass removal ($\Delta 2015$–2017; mean and standard error = 18% + −2%), with growth outpacing subsequent losses that occurred in 2020 and 2021 due to fire and mortality. Untreated groups maintained roughly the same amount of carbon between 2015 and 2019, but registered nearly a quarter reduction in carbon storage between 2019 and 2023 ($\sim -22\%$), largely a function of fire and mortality.

These patterns were present not only within grouped comparisons, but also when considered individually. Each

treatment was compared to its reference region to determine whether they produced a net-positive return on investment as measured by carbon (Figure 8). Reference regions strongly outperformed treatments between 2016 and 2019, but this pattern was quickly upended during 2020 and 2021 fire years; nearly 75% of treatments were outperforming their reference regions by 2023, at an average benefit of + 12.8 ± 4.7 Mg C ha^{-1} per treatment.

Discussion

The scope of the modern wildfire crisis demands rapid, landscape-scale evaluation of intervention effectiveness beyond what field-based monitoring alone can achieve. Our study demonstrates that integrating remote sensing with natural experimental design provides a powerful framework for assessing fuel treatment outcomes at ecologically meaningful scales. This approach aligns with recent calls to apply natural experiments and earth observation data to quantify resilience benefits across large, fire-prone landscapes (Hiers et al., 2020; Abatzoglou et al., 2021, Delacote et al., 2025).

This study contributes to the growing body of evidence demonstrating the efficacy of treatments in restoring climate- and disturbance-resilient forests, expanding these findings to a broader landscape scale. For example, Safford et al. (2012) showed that treatments in the Angora Fire region of the Lake Tahoe Basin reduced fire severity by 60%–70% compared to untreated areas, significantly decreasing the proportion of high-severity burns. Similarly, Stephens et al. (2009) reported that treatments lowered fire severity by reducing surface and ladder fuels, with treated areas experiencing 50% less tree mortality during subsequent wildfires in mixed-conifer forests. Building on this foundation, our results confirm similar outcomes across the Central Sierra Nevada, where treatments mitigated high-severity wildfire and stabilized carbon pools during extreme drought conditions. Our approach also extends the findings of these previous studies by providing a robust, generalizable framework for matching treatment-scale consolidated polygons (placebo treatment areas) and broader spatially disaggregated reference regions. Together, this approach and results reinforce the critical role of interventions near fire perimeter edges, where treatments effectively slowed the spread of megafires and reduced fire severity, demonstrating the scalability of these interventions across larger landscapes.

The placement and size of treatments mattered. Our analysis of effects along fire perimeters indicate that treatments were effective in reducing fire spread and severity, and that larger treatments were especially successful. This spatial pattern likely reflects both strategic planning and operational realities–treatments are often co-located with access infrastructure (e.g., roads; Greiner et al., 2025) and are frequently paired with suppression tactics (e.g., treatments are used as control points by firefighters working to suppress fires; Agee and Skinner, 2005). In other words, the placement of treatments is not random; treatments are often clustered together, with one treatment serving as a fuel break that extinguishes the fire before it can spread into another treated area (see Supplementary Figure 2). These findings support the idea that clustered, strategically placed treatments can act as effective firebreaks (Tubbesing et al., 2019), consistent with the economies

of scale argument put forward by Hunter and Taylor (2022). Importantly, treatments over 6 hectares in size were most effective, suggesting that larger-scale planning and implementation can yield far greater benefits.

While fire mitigation remains the central objective of most fuel treatments, our results reveal that thinning also conferred measurable resilience in the absence of fire. In unburned areas, treated forests continued to sequester aboveground live carbon during the severe 2020–2021 drought, while untreated forests stagnated or declined (Figure 5, Panel I – No Fire). Treated areas rebounded quickly once wetter conditions returned, regaining near-baseline carbon levels by 2023 despite the initial biomass removal. In contrast, untreated forests exhibited sustained carbon declines, suggesting that competition-driven vulnerability to drought limited their recovery. These patterns indicate that thinning may support not only fire resistance, but also physiological resilience to climatic stressors–including water limitation and heat-driven mortality (North et al., 2022).

The drought period captured in our study was among the most severe in recent decades. Palmer Drought Severity Index (PDSI) values for Placer County show that nearly half of 2020 exceeded moderate drought thresholds, compared to just six such months between 2016 and 2019 (Abatzoglou, 2013). The summer of 2020 was the driest on record across much of the southwestern U.S., and drought conditions extended well into 2021 under the influence of a La Niña event (Seager et al., 2022). That treated forests maintained or regained carbon stocks through this period underscores the importance of reducing structural overstocking to mitigate drought sensitivity and sustain long-term carbon uptake. Together, these results demonstrate that thinning treatments not only reduce fire severity and its carbon consequences but also bolster forests' capacity to withstand and recover from climate extremes. In a future defined by increasing aridity and disturbance, proactive forest management offers a credible pathway to stabilize carbon and maintain the ecological functions of Western mixed-conifer forests.

Like all remote sensing products, the NASA CMS Aboveground Biomass Product and remotely sensed CBI datasets used in this study contain inherent uncertainties (Kennedy et al., 2024). Although extensively validated using field data (Kennedy et al., 2018; Parks et al., 2019b; Duncanson et al., 2022), these products carry known limitations, particularly following disturbance events for biomass estimation. The NASA CMS biomass estimates are derived using an imputation-based approach that links FIA plot data with Landsat imagery–matching field plots to pixels using spectral and environmental similarity. While this method enables wall-to-wall estimation of forest attributes, Kennedy et al. (2018) highlight several limitations, including reduced accuracy in heterogeneous or structurally complex forests and increased uncertainty immediately after abrupt disturbances due to spectral ambiguity between biomass loss and early regrowth.

Additionally, though our study area is not among the high biomass forests known to saturate in remotely sensed products, effects can still reduce the sensitivity of estimates in denser stands, limiting the resolution of carbon change detection. These uncertainties are especially relevant in post-treatment and post-fire periods, where dynamic forest responses complicate remote estimation. In areas of high biomass, it is likely that losses from disturbance are muted by underestimations of pre-disturbance

conditions. Therefore, while our results show strong signals of treatment benefits even using conservative approaches to detect those signals, we emphasize that these are subject to known data constraints in biomass and fire severity estimation.

Causal inference and attribution in observational studies remains challenging (Fick et al., 2021), and requires additional scrutiny during study design and when interpreting results. In this study we conclude that the observed differences in Δcarbon across treatment and control groups can be attributed to the interaction of the implemented treatments and exposure to wildfire. Carbon dynamics are influenced by numerous factors, including unmeasured site conditions, past management history, and stochastic disturbance patterns from multiple causal agents. Our census-based matching approach was designed to reduce bias by ensuring reference regions shared similar ecological, climatic, and disturbance exposure characteristics, and the placebo component of our study design provides validation of match quality. The consistent patterns observed–specifically, strong carbon declines in burned areas and limited growth in unburned controls–were reproduced across all three untreated comparison groups. The consistency across these groups supports the interpretation that (1) treatment was the causal factor for the observed changes in carbon, and (2) treatment effects were real and not solely driven by sample size, location, or the stochastic nature of wildfire occurrence.

Analysis of the effectiveness of fuels treatments must be robust to uneven exposure because of the stochastic nature of wildfire across a landscape, the scale difference between treatment and potential reference areas, and the treatment effect on wildfire probability and spread all result in different exposure probabilities for the controls. Incorporating the analysis of placebo treatments enables testing for the consistency between placebo and reference region behavior. The lack of difference between the placebo and reference regions support the robustness of our counterfactual design, and increases confidence that observed differences in carbon retention stem from treatment effects rather than unmeasured confounders or random fire behavior (Supplementary Figure 4). This evidence against selection bias, combined with the subtracting out pre-treatment differences between regions, demonstrates that our results are not affected by the expected uneven exposure to wildfire between treatment and reference regions.

The placebo polygons, which mimic the siting criteria of real treatments but received no intervention, additionally provide indirect evidence that fuel treatment projects were strategically placed. These placebo polygons experienced more frequent and severe fire than their matched controls, highlighting the elevated risk in high-carbon, high-hazard areas left untreated. This suggests that our results may in fact represent a conservative estimate of treatment benefit, where comparisons between completed (treatment) and equivalent (placebo) projects would likely find a larger treatment effect. Moreover, the fact that pretreatment carbon levels in treated areas were higher than 93.5% of all measurements in the study domain indicates that managers successfully targeted overstocked, high-risk stands–a key consideration for future treatment prioritization strategies.

Our study aligns with a growing body of literature that challenges the perceived trade-off between carbon storage and fire risk reduction (e.g., Campbell et al., 2012; Law et al., 2022). In fact, our findings suggest that these goals are not only compatible but

potentially synergistic. Treatments that reduce fuels and enhance forest resilience can also stabilize carbon over decadal timescales. Further, treatments with a second entry (e.g., prescribed burns or biomass removal following initial thinning) performed even better– retaining more carbon while reducing fire severity more effectively (Figure 7).

Treatments which aim to increase resistance to wildfire actually result in forest resilience across multiple disturbances. A growing body of literature, including the research presented here, supports the idea that the efficacy of treatments depends on their intensity (i.e., amount of biomass removed per area) and configuration (size and placement on the landscape). Intensity of standard fuel mitigation treatments may currently be too low to achieve desired outcomes. For example, North et al. (2022) suggested that treatments should target "operational resilience," resulting in ∼25% more biomass removal than common practice. Likewise, configuration (location and size) of treatments has also been demonstrated to affect resistance to fire disturbance (McKinney et al., 2022; Urza et al., 2023; Ott et al., 2023), although the longer-term effects of configuration on resilience are not yet well understood. Similarly, in our work, we found that while some individual treatments failed to outperform their reference region in terms of both resistance and short- to mid-term resilience to disturbance, these treatments share key characteristics (i.e., small footprint, large distances from nearby treatments) that we suggest are at odds with successfully mitigating risk of high-severity fire. Promisingly, treatments in our study occurred prior to the roll-out of the Wildfire Crisis Strategy, which is now driving more landscape-scale, configuration-sensitive planning efforts. As a result, treatments that are being planned and implemented today are likely to be even more effective than the results presented here.

As climate change intensifies wildfires and drives crisis policy responses worldwide, it is critical to move beyond the false dichotomy pitting conservation against risk reduction. Ecological benefits provided by resilient landscapes, like durable live carbon storage, complex forest structures, and configurations essential for biodiversity, are not inherently at odds with treatments to reduce risk (Hjerpe et al., 2024, Long et al., 2021; Ritter et al., 2022). Indeed, proactive treatments, strategically placed, are likely to make carbon storage and key structure-dependent habitats for sensitive species more durable in the face of wildfire and drought (Restaino et al., 2019; Sitters and Di Stefano, 2020). Landscape-scale planning efforts that include broad groups of stakeholders, multiple ecosystem values and services, realistic fire risk, and treatment options can help quantify trade-offs and identify optimal treatment scenarios for restoring resilient landscapes. Tooling to support these complex, landscape-scale efforts is improving rapidly, and while further research can improve precision and performance of these tools, limits to action are more likely to be within the policy, public opinion, and financial realms. Embracing a wider lens on landscape management planning is critical: we must move from single projects focused on resistance to single disturbance agents, to multi-project efforts targeting resilience across sources of disturbance, and finally to landscape-scale resilience stewardship, where long-term initiatives enhance durability of ecosystem functions and services via ongoing management. This broadening of our mental model and ambition is a key paradigm shift needed to unlock action at scale.

Data availability statement

Code and data access are available via the following GitHub repo: https://github.com/Vibrant-Planet-Open-Science/Fire-Adapted-Forests.

Author contributions

EY: Writing – original draft, Conceptualization, Data curation, Formal analysis, Methodology, Software, Visualization. ME: Conceptualization, Methodology, Writing – review & editing, Investigation. JS: Methodology, Writing – review & editing, Formal analysis. SG: Writing – review & editing, Visualization. MK: Writing – review & editing, Data curation, Methodology, Resources. SP: Methodology, Writing – review & editing. MS: Writing – review & editing, Funding acquisition, Project administration. KD: Project administration, Writing – review & editing, Funding acquisition, Conceptualization, Formal analysis, Investigation, Methodology, Resources, Supervision, Visualization, Writing – original draft.

Funding

Acknowledgments

References

Abatzoglou, J. T. (2013). Development of gridded surface meteorological data for ecological applications and modelling. *Int. J. Climatol.* 33, 121–131. doi: 10.1002/joc.3413

Conflict of interest

ME was employed by Blue Forest. JS, MK and KD were employed by Vibrant Planet. SP was employed by Verra.

The remaining authors declare that the research was conducted in the absence of any commercial or financial relationships that could be construed as a potential conflict of interest.

The reviewer JS declared a shared affiliation with the author MS to the handling editor at time of review.

Publisher's note

All claims expressed in this article are solely those of the authors and do not necessarily represent those of their affiliated organizations, or those of the publisher, the editors and the reviewers. Any product that may be evaluated in this article, or claim that may be made by its manufacturer, is not guaranteed or endorsed by the publisher.

Supplementary material

The Supplementary Material for this article can be found online at: https://www.frontiersin.org/articles/10.3389/ffgc.2025.1498430/full#supplementary-material

SUPPLEMENTARY FIGURE 1
Example of a treatment polygon (blue) that has been repositioned on the landscape to simulate a "placebo" treatment. Black areas are pixels that meet our applicability criteria described in Table 2. Three failed placebo treatment placements (red) occur where equivalent treatment intervention polygons do not overlap with a sufficient number of applicability pixels. The green polygon, conversely occupies a high applicability area and is a sufficient placebo treatment. The conditions within the blue and green polygons vary, however, as shown in the adjacent plots.

SUPPLEMENTARY FIGURE 2
Example of treatment placement and its effects on fire severity along a northern border of the North Complex fire (2020).

SUPPLEMENTARY FIGURE 3
Comparison of fire prevalence regardless of source (e.g., prescribed burns and wildfire combined) across fire years for each treatment and non-treatment grouping.

SUPPLEMENTARY FIGURE 4
Results of carbon response and percentage of fire occurring on 10 replicate random drawings of placebo treatments and their reference regions. In each of the 10 iterations, placebos were matched with treatment polygons and randomly distributed in space until they met our applicability criteria. Top panel: placebos consistently had lower carbon stocks in 2023 than their reference regions, despite average carbon in 2015 being a matching criteria. The bottom panel shows that this behavior is directly tied to the amount of fire experienced in the two groupings; while reference regions are capable of reproducing fire trends across a broad area, placebos are limited to areas where carbon concentrations are comparable to treatment polygons. Such areas were especially prone to fire behavior during our study period.

Abatzoglou, J. T., Battisti, D. S., Williams, A. P., Hansen, W. D., Harvey, B. J. and Kolden, C. A. (2021). Projected increases in western US forest fire despite growing fuel constraints. *Commun. Earth Environ.* 2:227. doi: 10.1038/s43247-021-00299-0

Agee, J. K., and Skinner, C. N. (2005). Basic principles of forest fuel reduction treatments. *For. Ecol. Manage.* 211, 83–96. doi: 10.1016/j.foreco.2005.01.034

Arno, S. F., Scott, J. H., and Hartwell, M. G. (1995). *Age–Class Structure of Old-Growth Ponderosa Pine/Douglas-Fir Stands and its Relationship to Fire History.* Ogden, UT: USDA Forest Service.

Ashenfelter, O. C., and Card, D. (1984). Using the longitudinal structure of earnings to estimate the effect of training programs. *Rev. Econ. Statist.* 67, 648–660. doi: 10.2307/1924810

Badgley, G., Chay, F., Chegwidden, O. S., Hamman, J. J., Freeman, J., and Cullenward, D. (2022). California's forest carbon offsets buffer pool is severely undercapitalized. *Front. For. Glob. Change* 5:930426. doi: 10.3389/ffgc.2022.930426

Battocletti, V., Enriques, L., and Romano, A. (2024). The voluntary carbon market: Market failures and policy implications. *U. Colo. L. Rev.* 95:519. doi: 10.2139/ssrn.4380899

Bentz, B. J., Regniere, J., Fettig, C. J., Hansen, E. M., Hayes, J. L., Hicke, J. A., et al. (2010). Climate change and bark beetles of the western United States and Canada: Direct and indirect effects. *BioScience* 60, 602–613. doi: 10.1525/bio.2010.60.8.6

Breiman, L. (2001). Random Forests. *Mach. Learn.* 45, 5–32. doi: 10.1023/A:1010950718922

Brown, R. T., Agee, J. K., and Franklin, J. F. (2004). Forest restoration and fire: Principles in the context of place. *Conserv. Biol.* 18, 903–912. doi: 10.1111/j.1523-1739.2004.521_1.x

CalFire (2024). *California Multi-Source Land Ownership.* Sacramento, CA: California Department of Forestry and Fire Protection.

Campbell, J. L., Harmon, M. E., and Mitchell, S. R. (2012). Can fuel-reduction treatments really increase forest carbon storage in the western US by reducing future fire emissions? *Front. Ecol. Environ.* 10, 83–90. doi: 10.2307/41480005

Chu, L., Grafton, R. Q., and Nelson, H. (2023). Accounting for forest fire risks: Global insights for climate change mitigation. *Mitig. Adapt. Strateg. Glob. Change* 28:48. doi: 10.1007/s11027-023-10087-0

Coop, J. D., Parks, S. A., McClernan, S. R., and Holsinger, L. M. (2016). Influences of prior wildfires on vegetation response to subsequent fire in a reburned Southwestern landscape. *Ecol. Appl.* 26, 346–354. doi: 10.1890/15-0775

Coop, J. D., Parks, S. A., Stevens-Rumann, C. S., Crausbay, S. D., Higuera, P. E., Hurteau, M. D., et al. (2020). Wildfire-driven forest conversion in western North American landscapes. *BioScience* 70, 659–673. doi: 10.1093/biosci/biaa061

Coop, J. D., Parks, S. A., Stevens-Rumann, C. S., Ritter, S. M., and Hoffman, C. M. (2022). Extreme fire spread events and area burned under recent and future climate in the western USA. *Global Ecology and Biogeography* 31, 1949–1959. doi: 10.1111/geb.13496

Dale, V. H., Joyce, L. A., McNulty, S., Neilson, R. P., Ayres, M. P., Flannigan, M. D., et al. (2001). Climate change and forest disturbances: Climate change can affect forests by altering the frequency, intensity, duration, and timing of fire, drought, introduced species, insect and pathogen outbreaks, hurricanes, windstorms, ice storms, or landslides. *BioScience* 51, 723–734. doi: 10.1641/0006-35682001051[0723:CCAFD]2.0.CO;2

Davis, K. T., Dobrowski, S. Z., Higuera, P. E., Holden, Z. A., Veblen, T. T., Rother, M. T., et al. (2019). Wildfires and climate change push low-elevation forests across a critical climate threshold for tree regeneration. *Proc. Natl. Acad. Sci.* 116, 6193–6198. doi: 10.1073/pnas.181510711

Davis, K. T., Peeler, J., Fargione, J., Haugo, R. D., Metlen, K. L., Robles, M. D., et al. (2024). Tamm review: A meta-analysis of thinning, prescribed fire, and wildfire effects on subsequent wildfire severity in conifer dominated forests of the Western U.S. *For. Ecol. Manage.* 561:121885. doi: 10.1016/j.foreco.2024.121885

Davis, K. T., Robles, M. D., Kemp, K. B., Higuera, P. E., Chapman, T., Metlen, K. L., et al. (2023). Reduced fire severity offers near-term buffer to climate-driven declines in conifer resilience across the western United States. *Proc. Natl. Acad. Sci.* 120:e2208120120. doi: 10.1073/pnas.2208120120

Delacote, P., Chabé-Ferret, S., Creti, A., Duffy, K., Elias, M., Groom, B., et al. (2025). Restoring credibility in carbon offsets through systematic *ex post* evaluation. *Nat. Sustain.* 8, 733–740. doi: 10.1038/s41893-025-01589-7

Dillon, G. K. (2015). *Wildfire Hazard Potential (WHP) for the conterminous United States (270-m GRID), version 2014 Continuous.* Salt Lake City, UT: Forest Service Research Data Archive.

Duncanson, L., Kellner, J., Armston, J., Dubayah, R., Minor, D., Hancock, S., et al. (2022). Aboveground biomass density models for NASA's Global Ecosystem Dynamics Investigation (GEDI) lidar mission. *Remote Sens. Environ.* 270:112845. doi: 10.1016/j.rse.2021.112845

Elias, M., Yackulic, E., Duffy, K., Saksa, P., Sanchez, D. L., Pevzner, N., et al. (2025). Carbon finance for forest resilience in California. *Front. For. Glob. Change* 7:1507554. doi: 10.3389/ffgc.2024.1507554

Fettig, C. J., Mortenson, L. A., Bulaon, B. M., and Foulk, P. B. (2019). Tree mortality following drought in the central and southern Sierra Nevada, California, US. *For. Ecol. Manage.* 432, 164–178. doi: 10.1016/j.foreco.2018.09.006

Fick, S. E., Nauman, T. W., Brungard, C. C., and Duniway, M. C. (2021). Evaluating natural experiments in ecology: using synthetic controls in assessments of remotely sensed land treatments. *Ecol. Appl.* 31:e02264. doi: 10.1002/eap.2264.

Fites-Kaufman, J., Rundel, P., Stephenson, N., and Weixelman, D. A. (2007). Montane and subalpine vegetation of the Sierra Nevada and Cascade ranges. *Red* 159, 456–501. doi: 10.1525/california/9780520249554.003.0017

Golmant, N., Morrissey, M., Silva, C., Dorrek, F., and Engstrand, R. (2023). *Assessing Forest Carbon Offset Additionality with Dynamic Baselines and Uncertainty Quantification.* Chennai: Pachama.

Greiner, S. M., Schultz, C., Novak, K. M., and Lohman, A. (2025). The role of fuel treatments during incident management. *Fire Ecol.* 21:25. doi: 10.1186/s42408-025-00369-0

Hessburg, P. F., Churchill, D. J., Larson, A. J., Haugo, R. D., Miller, C., Spies, T. A., et al. (2015). Restoring fire-prone Inland Pacific landscapes: Seven core principles. *Landsc. Ecol.* 30, 1805–1835. doi: 10.1007/s10980-015-0218-0

Hessburg, P. F., Miller, C. L., Parks, S. A., Povak, N. A., Taylor, A. H., Higuera, P. E., et al. (2019). Climate, environment, and disturbance history govern resilience of western North American forests. *Front. Ecol. Evol.* 7:239. doi: 10.3389/fevo.2019.00239

Hiers, J. K., O'Brien, J. J., Varner, J. M., Butler, B., Dickinson, M., Hood, S., et al. (2020). Prescribed fire science: The case for a refined research agenda. *Fire Ecol.* 16:11. doi: 10.1186/s42408-019-0046-8

Hijmans, R. (2025). *Terra: Spatial Data Analysis. R package version 1.8-61.* Available online at: https://github.com/rspatial/terra (accessed January 30, 2022).

Hjerpe, E. E., Colavito, M., Waltz, A., and Sánchez Meador, A. (2024). Return on investments in restoration and fuel treatments in frequent-fire forests of the American west: A meta-analysis. *Ecol. Econ.* 223:108244. doi: 10.1016/j.ecolecon.2024.108244

Hunter, M. E., and Taylor, M. H. (2022). The economic value of fuel treatments: A review of the recent literature for fuel treatment planning. *Forests* 13:2042. doi: 10.3390/f13122042

Hurteau, M. D., Goodwin, M. J., Marsh, C., Zald, H. S., Collins, B., Meyer, M., et al. (2024). Managing fire-prone forests in a time of decreasing carbon carrying capacity. *Front. Ecol. Environ.* 22:e2801. doi: 10.1002/fee.2801

Hurteau, M. D., Liang, S., Westerling, A. L., and Wiedinmyer, C. (2019). Vegetation-fire feedback reduces projected area burned under climate change. *Sci. Rep.* 9:2838. doi: 10.1038/s41598-019-39284-1

IPCC (2006). *2006 IPCC Guidelines for National Greenhouse Gas Inventories: Volume 4 – Agriculture, Forestry and Other Land Use.* Geneva: Intergovernmental Panel on Climate Change

Kelly, L. T., and Brotons, L. (2017). Using fire to promote biodiversity. *Science* 355, 1264–1265. doi: 10.1126/science.aam7672

Kennedy, R., Kane, V., and Powell, S. (2024). *Integrating and Expanding a Regional Carbon Monitoring System into the NASA CMS Forest biomass maps.* Available online at: https://carbon.nasa.gov/cgi-bin/inv_pgp.pl?pgid=656&format=1 (accessed November 29, 2018).

Kennedy, R. E., Ohmann, J., Gregory, M., Roberts, H., Yang, Z., Bell, D. M., et al. (2018). An empirical, integrated forest biomass monitoring system. *Environ. Res. Lett.* 13:025004. doi: 10.1088/1748-9326/aa9d9e

Knight, C. A., Tompkins, R. E., Wang, J. A., York, R., Goulden, M. L., and Battles, J. J. (2022). Accurate tracking of forest activity key to multi-jurisdictional management goals: A case study in California. *J. Environ. Manage.* 302(Pt B):114083. doi: 10.1016/j.jenvman.2021.114083.

Koontz, M. J., Latimer, A. M., Mortenson, L. A., Fettig, C. J., and North, M. P. (2021). Cross-scale interaction of host tree size and climatic water deficit governs bark beetle-induced tree mortality. *Nat. Commun.* 12:129. doi: 10.1038/s41467-020-20455-y

Koontz, M. J., North, M. P., Werner, C., Fick, S., and Latimer, A. (2020). Local forest structure variability increases resilience to wildfire in dry western US coniferous forests. *Ecol. Lett.* 23, 483–494. doi: 10.1111/ele.13447.

Kruschke, J. K. (2018). Rejecting or accepting parameter values in Bayesian estimation. *Adv. Methods Pract. Psychol. Sci.* 1:251524591877130. doi: 10.1177/2515245918771304

Landfire (2014). *Existing Vegetation Cover, LANDFIRE 1.4.0, U.S. Department of the Interior, Geological Survey, and U.S. Department of Agriculture.* Washington, DC: U.S. Department of Agriculture

Landfire (2016). *Existing Vegetation Type, LANDFIRE 2.0.0, U.S. Department of the Interior, Geological Survey, and U.S. Department of Agriculture.* Washington, DC: U.S. Department of Agriculture.

Larson, A. J., and Churchill, D. (2012). Tree spatial patterns in fire-frequent forests of western North America, including mechanisms of pattern formation and implications for designing fuel reduction and restoration treatments. *For. Ecol. Manage.* 267, 74–92. doi: 10.1016/j.foreco.2011.11.038

Law, B. E., Moomaw, W. R., Hudiburg, T. W., Schlesinger, W. H., Sterman, J. D., and Woodwell, G. M. (2022). Creating strategic reserves to protect forest carbon and reduce biodiversity losses in the United States. *Land* 11:721. doi: 10.3390/land11050721

Long, J. W., Lake, F. K., and Goode, R. W. (2021). The importance of Indigenous cultural burning in forested regions of the Pacific West, USA. *For. Ecol. Manage.* 500:119597. doi: 10.1016/j.foreco.2021.119597

Makowski, D., Ben-Shachar, M. S., and Lüdecke, D. (2019). bayestestR: Describing effects and their uncertainty, existence and significance within the Bayesian framework. *J. Open Source Softw.* 4:1541. doi: 10.21105/joss.01541

McDowell, N., Pockman, W. T., Allen, C. D., Breshears, D. D., Cobb, N., Kolb, T., et al. (2008). Mechanisms of plant survival and mortality during drought: Why do some plants survive while others succumb to drought? *New Phytol.* 178, 719–739. doi: 10.1111/j.1469-8137.2008.02436.x

McKinney, S. T., Abrahamson, I., Jain, T., and Anderson, N. (2022). A systematic review of empirical evidence for landscape-level fuel treatment effectiveness. *Fire Ecol.* 18:21. doi: 10.1186/s42408-022-00146-3

Millar, C. I., and Stephenson, N. L. (2015). Temperate forest health in an era of emerging megadisturbance. *Science* 349, 823–826. doi: 10.1126/science.aaa9933

North, M. P., Tompkins, R. E., Bernal, A. A., Collins, B. M., Stephens, S. L., and York, R. A. (2022). Operational resilience in western US frequent-fire forests. *Forest Ecol. Manage.* 507:120004. doi: 10.1016/j.foreco.2021.120004

Omernik, J. M., and Griffith, G. E. (2014). Ecoregions of the conterminous United States: Evolution of a hierarchical spatial framework. *Environ. Manage.* 54, 1249–1266. doi: 10.1007/s00267-014-0364-1

Ott, J. E., Kilkenny, F. F., and Jain, T. B. (2023). Fuel treatment effectiveness at the landscape scale: A systematic review of simulation studies comparing treatment scenarios in North America. *Fire Ecol.* 19:10. doi: 10.1186/s42408-022-00163-2

Ouzts, J., Kolb, T., Huffman, D., and Sánchez Meador, A. (2015). Post-fire ponderosa pine regeneration with and without planting in Arizona and New Mexico. *For. Ecol. Manage.* 354, 281–290. doi: 10.1016/j.foreco.2015.06.001

Parks, S. A., Dobrowski, S. Z., Shaw, J. D., and Miller, C. (2019a). Living on the edge: Trailing edge forests at risk of fire-facilitated conversion to non-forest. *Ecosphere* 10:e02651. doi: 10.1002/ecs2.2651

Parks, S. A., Holsinger, L. M., Koontz, M. J., Collins, L., Whitman, E., Parisien, M. A., et al. (2019b). Giving ecological meaning to satellite-derived fire severity metrics across North American forests. *Remote Sensing* 11:1735. doi: 10.3390/rs11141735

Parks, S. A., Holsinger, L. M., Blankenship, K., Dillon, G. K., Goeking, S. A., and Swaty, R. (2023). Contemporary wildfires are more severe compared to the historical reference period in western US dry conifer forests. *For. Ecol. Manage.* 544:121232. doi: 10.1016/j.foreco.2023.121232

Parks, S. A., Holsinger, L. M., Panunto, M. H., Jolly, W. M., Dobrowski, S. Z., and Dillon, G. K. (2018). High-severity fire: Evaluating its key drivers and mapping its probability across western US forests. *Environ. Res. Lett.* 13:044037. doi: 10.1088/1748-9326/aab791

Parks, S. A., Miller, C., Abatzoglou, J. T., Holsinger, L. M., Parisien, M. A., and Dobrowski, S. Z. (2016). How will climate change affect wildland fire severity in the western U.S. *Environ. Res. Lett.* 11:035002. doi: 10.1088/1748-9326/11/3/035002

Radeloff, V. C., Helmers, D. P., Mockrin, M. H., Carlson, A. R., Hawbaker, T. J., and Martinuzzi, S. (2023). *The 1990-2020 Wildland-Urban Interface of the Conterminous United States - Geospatial Data*, 4th Edn. Fort Collins, CO: Forest Service Research Data Archive.

Restaino, C. M., Young, D. J., Estes, B., Gross, S. E., Wuenschel, A., Meyer, M. D., et al. (2019). Forest structure and climate mediate drought-induced tree mortality in forests of the Sierra Nevada, USA. *Ecol. Appl.* 29:e01902. doi: 10.1002/eap.1902

Ritter, S. M., Hoffman, C. M., Battaglia, M. A., and Jain, T. B. (2022). Restoration and fuel hazard reduction result in equivalent reductions in crown fire behavior in dry conifer forests. *Ecol. Appl.* 32:e2682. doi: 10.1002/eap.2682

Safford, H. D., Paulson, A. K., Steel, Z. L., Young, D. J., and Wayman, R. B. (2022). The 2020 California fire season: A year like no other, a return to the past or a harbinger of the future? *Glob. Ecol. Biogeogr.* 31, 2005–2025. doi: 10.1111/geb.13498

Safford, H. D., and Stevens, J. T. (2017). *Natural Range of Variation for Yellow Pine and Mixed-Conifer Forests in the Sierra Nevada, southern Cascades, and Modoc and Inyo National Forests, California, USA*. Albany, CA: U.S. Department of Agriculture.

Safford, H. D., Stevens, J. T., Merriam, K., Meyer, M. D., and Latimer, A. M. (2012). Fuel treatment effectiveness in California yellow pine and mixed conifer forests. *For. Ecol. Manage.* 274, 17–18. doi: 10.1016/j.foreco.2012.02.013

Savage, M., and Mast, J. (2005). How resilient are Southwestern ponderosa pine forests after crown fires? *Can. J. For. Res.* 35, 967–977. doi: 10.1139/x05-028

Seager, R., Ting, M., Alexander, P., Nakamura, J., Liu, H., Li, C., et al. (2022). Mechanisms of a meteorological drought onset: Summer 2020 to spring 2021 in Southwestern North America. *J. Clim.* 35, 7367–7385. doi: 10.1175/JCLI-D-22-0314.1

Sitters, H., and Di Stefano, J. (2020). Integrating functional connectivity and fire management for better conservation outcomes. *Conserv. Biol.* 34, 550–560. doi: 10.1111/cobi.13446.

Steel, Z. L., Koontz, M. J., and Safford, H. D. (2018). The changing landscape of wildfire: Burn pattern trends and implications for California's yellow pine and mixed conifer forests. *Landsc. Ecol.* 33, 1159–1176. doi: 10.1007/s10980-018-0665-5

Stephens, S. L., Moghaddas, J. J., Edminster, C., Fiedler, C. E., Haase, S., Harrington, M., et al. (2009). Fire treatment effects on vegetation structure, fuels, and potential fire severity in western US forests. *Ecol. Appl.* 19, 305–320. doi: 10.1890/07-1755.1

Stevens-Rumann, C. S., Kemp, K. B., Higuera, P. E., Harvey, B. J., Rother, M. T., Donato, D. C., et al. (2018). Evidence for declining forest resilience to wildfires under climate change. *Ecol. Lett.* 21, 243–252. doi: 10.1111/ele.12889

Tubbesing, C. L., Fry, D. L., Roller, G. B., Collins, B. M., Fedorova, V. A., Stephens, S. L., et al. (2019). Strategically placed landscape fuel treatments decrease fire severity and promote recovery in the northern Sierra Nevada. *For. Ecol. Manage.* 436, 45–55. doi: 10.1016/j.foreco.2019.01.010

Urza, A. K., Hanberry, B. B., and Jain, T. B. (2023). Landscape-scale fuel treatment effectiveness: Lessons learned from wildland fire case studies in forests of the western United States and Great Lakes region. *Fire Ecol.* 19:1. doi: 10.1186/s42408-022-00159-y

Van de Water, K. M., and Safford, H. D. (2011). A summary of fire frequency estimates for California vegetation before Euro-American settlement. *Fire Ecol.* 7, 26–58. doi: 10.4996/fireecology.0703026

Welty, J., and Jeffries, M. (2021). *Combined Wildland Fire Datasets for the United States and Certain Territories, 1800s-Present: US Geological Survey data release*. Corvallis, OR: US Geological Survey.

West, T. A., Wunder, S., Sills, E. O., Börner, J., Rifai, S. W., Neidermeier, A. N., et al. (2023). Action needed to make carbon offsets from forest conservation work for climate change mitigation. *Science* 381, 873–877. doi: 10.1126/science.ade3535

WFMRDA Interagency Wildland Fire Perimeter History (2022). *Wildland Fire Management Research, Development and Application Interagency Wildland Fire Perimeter History*. Available online at: https://data-nifc.opendata.arcgis.com/datasets/nifc::interagencyfireperimeterhistory-all-years-view/about (accessed December 12, 2023).

Williams, J. N., Safford, H. D., Enstice, N., Steel, Z. L., and Paulson, A. K. (2023). High-severity burned area and proportion exceed historic conditions in Sierra Nevada, California, and adjacent ranges. *Ecosphere* 14:e4397. doi: 10.1002/ecs2.4397